


PI-RADS: Where Next?

Baris Turkbey, MD • Andrei S. Purysko, MD

From the Molecular Imaging Branch, National Cancer Institute, National Institutes of Health, 10 Center Dr, MSC 1182, Building 10, Room B3B85, Bethesda, MD 20892 (B.T.); and Section of Abdominal Imaging, Department of Nuclear Radiology, Cleveland Clinic Imaging Institute, Cleveland, Ohio (A.S.P.). Received December 7, 2022; revision requested December 26; revision received February 6, 2023; accepted February 13. Address correspondence to B.T. (email: turkbey@mail.nih.gov).

Conflicts of interest are listed at the end of this article.

See also the review “Adnexal Lesion Imaging: Past, Present, and Future” by Sadowski et al in this issue.

Radiology 2023; 307(5):e223128 • <https://doi.org/10.1148/radiol.223128> • Content codes: 

Prostate MRI plays an important role in the clinical management of localized prostate cancer, mainly assisting in biopsy decisions and guiding biopsy procedures. The Prostate Imaging Reporting and Data System (PI-RADS) has been available to radiologists since 2012, with the most up-to-date and actively used version being PI-RADS version 2.1. This review article discusses the current use of PI-RADS, including its limitations and controversies, and summarizes research that aims to improve future iterations of this system.

© RSNA, 2023

It has been 40 years since the first report of MRI for the care of patients with prostate cancer (PCa) (1). Its use was mainly limited to local staging in the first 3 decades, whereas detecting lesions and guiding biopsies have been the primary clinical uses in the past decade. Despite data showing the benefit of using MRI guidance for PCa diagnosis, prostate MRI was prone to wide variations between practices, which inevitably resulted in variations in diagnostic performance (2). While several factors contributed to performance variations (eg, the pretest risk probability of the patient population imaged, MRI equipment), unintentional reader inconsistency associated with subjective evaluation criteria and methods was documented as a substantial source of variation in the early 2010s (3,4). This resulted in a consensus document in 2012 aimed at bringing uniformity to prostate MRI acquisition and interpretation (5). That document was well received but not widely adopted by the radiology community and was mainly used as a clinical guideline for European radiologists. This document included key information about image acquisition and interpretation of each MRI pulse sequence, along with a tiered five-category system to determine the risk of clinically significant PCa (csPCa) with use of each MRI sequence. Most importantly, it included the word “PI-RADS,” one of the first occasions in which the “RADS” approach was proposed in the radiology literature beyond breast imaging. This document later became known as the Prostate Imaging Reporting and Data System (PI-RADS) version 1. Its adoption was hampered by a lack of clear guidance on how to derive the final risk assessment categories for individual lesions.

In late 2014, PI-RADS version 2 was released as a joint venture of the European Society of Urogenital Radiology and the American College of Radiology with support from the AdMeTech Foundation (6). In contrast with its first version, PI-RADS version 2 recommended having one overall score for each lesion based on all MRI sequences, and it also had more robust international representation in the expert panel, leading to rapid adoption by the radiology and urology communities. Several prospective and retrospective studies assessing

the performance of the system were subsequently conducted with favorable results compared with the first version (7). Based on the findings of those studies, an updated version (PI-RADS version 2.1) was released in 2019 and is currently in use (8).

In this review, we discuss the current use of PI-RADS, including its limitations and controversies, and summarize research that highlights opportunities to improve future versions.

PI-RADS Application and System Performance

The primary use of PI-RADS is for the detection and localization of csPCa in treatment-naïve men, irrespective of the prior prostate biopsy results. In PI-RADS version 2, csPCa was defined as “Gleason score ≥ 7 (including 3+4 with prominent but not predominant Gleason 4 component), and/or volume ≥ 0.5 cc, and/or extra prostatic extension.” However, studies evaluating the performance of PI-RADS define csPCa as any cancer with a Gleason score of 7 or higher. This simplified definition is in line with current guidelines (9,10), which do not consider Gleason 6 tumors to be csPCa, even when they have a high volume, and is used herein.

The use of PI-RADS scores to determine the need for prostate biopsy has been reported on extensively. It is supported by level 1 evidence that shows that, compared with standard transrectal US-guided biopsy, MRI examinations interpreted using PI-RADS can increase the detection of csPCa while mitigating overdiagnosis of insignificant cancer and reducing the number of unnecessary biopsies. In the pivotal PRECISION (Prostate Evaluation for Clinically Important Disease: Sampling Using Image Guidance or Not?) trial, 500 participants from 25 centers underwent randomization into two arms. In the MRI-targeted biopsy arm, 252 participants underwent prostate MRI, of whom 181 had PI-RADS category 3 or higher lesions and underwent MRI-targeted prostate biopsy. In the standard biopsy arm, 248 participants underwent systematic transrectal US-guided biopsy procedures without undergoing pre-biopsy MRI. In the MRI-targeted biopsy arm, csPCa

Abbreviations

ADC = apparent diffusion coefficient, AI = artificial intelligence, AUC = area under the receiver operating characteristic curve, bpMRI = biparametric MRI, csPCa = clinically significant PCa, DCE = dynamic contrast-enhanced, DWI = diffusion-weighted imaging, mpMRI = multiparametric MRI, PCa = prostate cancer, PI-QUAL = Prostate Imaging Quality, PI-RADS = Prostate Imaging Reporting and Data System, PSA = prostate-specific antigen

Summary

Emerging risk prediction models, quantitative MRI methods, and sophisticated artificial intelligence systems, along with rigorous quality control processes, can potentially improve the performance of the Prostate Imaging Reporting and Data System for the detection of clinically significant prostate cancer.

Essentials

- Prostate MRI is commonly used to guide biopsies in men with an increased risk of clinically significant prostate cancer (csPCa).
- Despite its subjectiveness, the Prostate Imaging Reporting and Data System (PI-RADS) is useful in detecting csPCa suspicious lesions and assisting biopsy decisions.
- The use of risk prediction models, quantitative MRI methods, and artificial intelligence may improve the performance of PI-RADS.
- Quality control is necessary to mitigate variations in prostate MRI quality and will be critical to the implementation of biparametric MRI protocols.

was detected in 38% of participants versus 26% in the systematic biopsy arm ($P = .005$), whereas insignificant PCa was detected in 9% of participants in the MRI arm versus 22% in the systematic biopsy arm ($P < .0001$) (11). In another multicenter randomized clinical trial conducted in Canada, 453 participants were randomized to two arms (12). In arm 1, 226 patients underwent systematic biopsy, whereas in arm 2, 227 patients underwent MRI and MRI-targeted biopsy. In arm 1, csPCa was detected in 30% of participants versus 35% in arm 2. The study results indicated that 37% of participants had negative MRI results and could have avoided undergoing a prostate biopsy.

The high negative predictive value of MRI for csPCa with use of PI-RADS has also been demonstrated in the PCa screening setting, where the prevalence of csPCa is lower than in the population with clinical suspicion for PCa typically referred for MRI (13,14). In a population-based trial conducted in Sweden, MRI-based screening was found to reduce the number of both lifetime biopsies and overdiagnosis of insignificant cancer by 50% compared with traditional prostate-specific antigen (PSA) screening followed by reflex biopsy (15).

While prostate MRI and MRI-guided interventions using PI-RADS significantly improve csPCa detection compared with standard US-guided biopsy (Fig 1), a nonnegligible number of csPCa are missed at MRI (16). Some of these cancers have an appearance that either resembles benign lesions or does not fit well into the categories described in PI-RADS (Figs 2, 3). There are, however, cancers that are less conspicuous at prostate MRI using the current techniques described in PI-RADS. This is increasingly recognized with the advent of prostate-specific membrane antigen–targeted PET/CT radioligands, which can

reveal some of these “MRI-invisible” lesions (Fig 4) (17). Conversely, several conditions, such as benign prostatic hyperplasia, prostatitis, and atrophy, can mimic PCa at MRI and lead to an unnecessary biopsy (Fig 5).

Therefore, besides adjustments in PI-RADS, additional strategies will be necessary to improve the detection of csPCa while also further decreasing the detection of insignificant cancers, ideally reducing the interobserver variability in prostate MRI interpretation, which continues to be a source of variability in MRI performance in the PI-RADS era (2).

Inclusion of PI-RADS in PCa Risk Prediction Models

PI-RADS assessment categories communicate the probability of the presence of csPCa solely based on MRI findings. There is, however, a growing body of literature on developing statistical models to improve the ability to predict which patients may have csPCa by using PI-RADS scores combined with clinical and laboratory data.

Radtke et al (18) developed a risk model that included PSA levels, prostate volume, digital rectal examination, and PI-RADS version 1–based prebiopsy MRI data from 1159 patients, which successfully predicted patients who had csPCa at prostate biopsy. When this risk model was combined with the European Randomized Study of Screening for Prostate Cancer, or ERSPC, risk calculator, it performed better than the risk calculator alone (area under the receiver operating characteristic curve [AUC], 0.84 vs 0.81).

In a study by Mehravand et al (19), a model was developed to predict the presence of csPCa at biopsy based on the patient's age, ethnicity, prostate volume, PSA density (ie, serum PSA divided by gland volume), and PI-RADS categories in a cohort of 400 men. In an external validation cohort, the model predicted patients with an increased risk of csPCa better than a model that did not include any imaging information (AUC, 0.84 vs 0.64). Additionally, this model avoided 18% of unnecessary biopsies at a risk threshold of 20% without missing any csPCa diagnosis in a decision curve analysis.

Among clinical parameters, PSA density is the one that has been used most often and shown to be a valuable method to identify patients who would benefit from undergoing biopsy when the MRI results are either negative or indeterminate (ie, PI-RADS category ≤ 3) (20). In a retrospective analysis by Deniffel et al (21), clinical and MRI data of 385 patients were used to test four prostate biopsy prediction models and compare them against a more straightforward model developed by the authors, which uses PI-RADS version 2 and PSA density. Up to a risk threshold of 15%, the four models performed worse than the authors' prediction model using PI-RADS version 2 and PSA density, which was documented to have avoided 6.3% of unnecessary prostate biopsies (21).

Improving Objectivity of PI-RADS with Use of Quantitative Methods

One of the main limitations of PI-RADS is the subjective definitions used to assign the different categories to detected lesions. The subjective definitions include three groups: shape (eg, linear, wedge,

round, lenticular), signal intensity (eg, mild, moderate, markedly hypointense or hyperintense), and lesion boundaries (eg, completely or mostly encapsulated, obscured margins). Different combinations of these three groups are used for category assignment of detected lesions, making it challenging to achieve high levels of interobserver and intraobserver agreement (Tables 1–4). Ultimately, this negatively impacts critical interventional decisions, such as biopsy.

Quantitative MRI methods have been used in clinical care for at least 2 decades. The readily quantifiable pulse sequences for prostate MRI are diffusion-weighted imaging (DWI) and dynamic contrast-enhanced (DCE) imaging. Currently, PI-RADS does not endorse quantification for these two pulse sequences for imaging interpretation, partly due to reproducibility concerns (22). However, this is an active area of research, and some published results indicate metrics that should be further explored to improve prostate MRI accuracy and reduce interobserver variability.

In a study by Gaur et al (23) with 100 patients who underwent prostatectomy, apparent diffusion coefficient (ADC) values normalized by the ADC values of benign prostatic tissue in the same zone were used to optimize PI-RADS categorization of lesions detected at prostate MRI. The AUCs for ADC and normalized ADC were 87% and 82%, respectively, for predicting reader PI-RADS category 4 or 5 lesions. An ADC of less than $1.06 \times 10^{-3} \text{ mm}^2/\text{sec}$ and a normalized ADC of less than 0.65 achieved positive predictive values of 83% and 84% for the correct classification of PI-RADS version 2 category 1–3 versus category 4–5 lesions, respectively. These results were valid in both peripheral and transition zone lesions.

In a more recent study, Tavakoli et al (24) found several quantitative parameters from DCE imaging, ADC maps, and normalized T2 values to be predictive of cPca. ADCs were the most robust parameter, and a value of $0.90 \times 10^{-3} \text{ mm}^2/\text{sec}$ or less supported the upgrading of DWI and ADC PI-RADS 3 ($P = .007$) and DWI and ADC PI-RADS 4 ($P < .001$) lesions, while DCE imaging parameters did not.

Opportunities for Artificial Intelligence

Artificial intelligence (AI) is a trendy research topic in medical imaging fueled by the increased availability of graphical processing unit computers and integrated development environments. AI methods are currently used for prostate gland

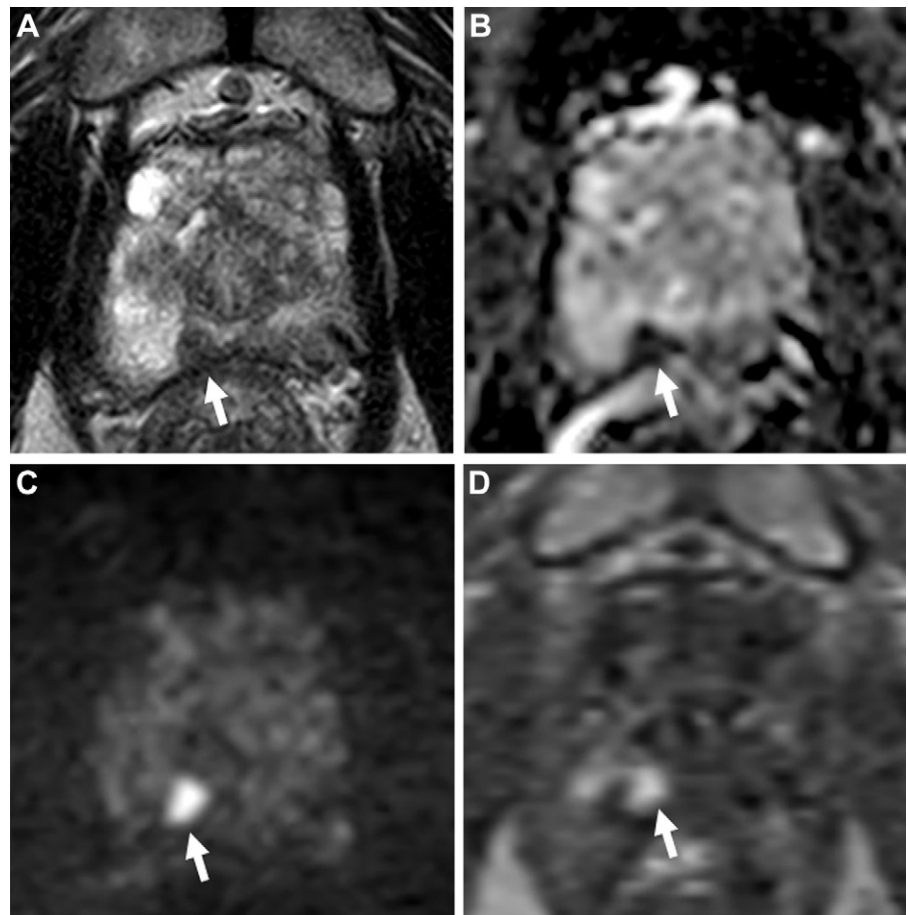


Figure 1: Images in a 70-year-old man with a serum prostate-specific antigen level of 6.8 ng/mL. **(A)** Axial T2-weighted MRI scan shows a focal hypointense lesion in the right apical peripheral zone (arrow). **(B)** Apparent diffusion coefficient map and **(C)** diffusion-weighted image with a b value of $1500 \text{ sec}/\text{mm}^2$ show a lesion with diffusion restriction with prominent hypointense and hyperintense signal features (arrows), and **(D)** dynamic contrast-enhanced (DCE) MRI scan shows focal early enhancement (arrow). The T2-weighted imaging, diffusion-weighted imaging, DCE MRI, and overall Prostate Imaging Reporting and Data System (PI-RADS) scores of this lesion were 4, 4, positive, and 4, respectively. Transrectal US/MRI fusion-guided biopsy with a transperineal approach revealed Gleason 3+4 prostate cancer with cribriform pattern within this PI-RADS category 4 lesion.

segmentation in clinical practice for gland volume calculation and preparation for MRI-guided biopsy. Recently, there has been a growing interest in expanding the use of AI models to many other applications, from imaging acquisition to reporting. Concerning PCa detection, early data shows that these AI models can potentially increase the radiologists' efficiency by reducing the imaging interpretation time by means of automated lesion detection, increase the readers' accuracy—especially for those less experienced—and improve interobserver agreement (25) (Figs 6, 7).

The reported performance of AI models for PCa detection approaches—and in some cases, surpasses—the performance of human readers. A higher performance level, however, appears to be achieved by combining radiologists and AI models. In a systematic review (26), AI models' average sensitivity and specificity were 84% and 61.5%, respectively. In a subsequent analysis, the pooled sensitivity and specificity of radiologists with AI assistance were 89.1% and 78.1%, respectively, compared with 79.5% and 73.1% for radiologists alone (27).

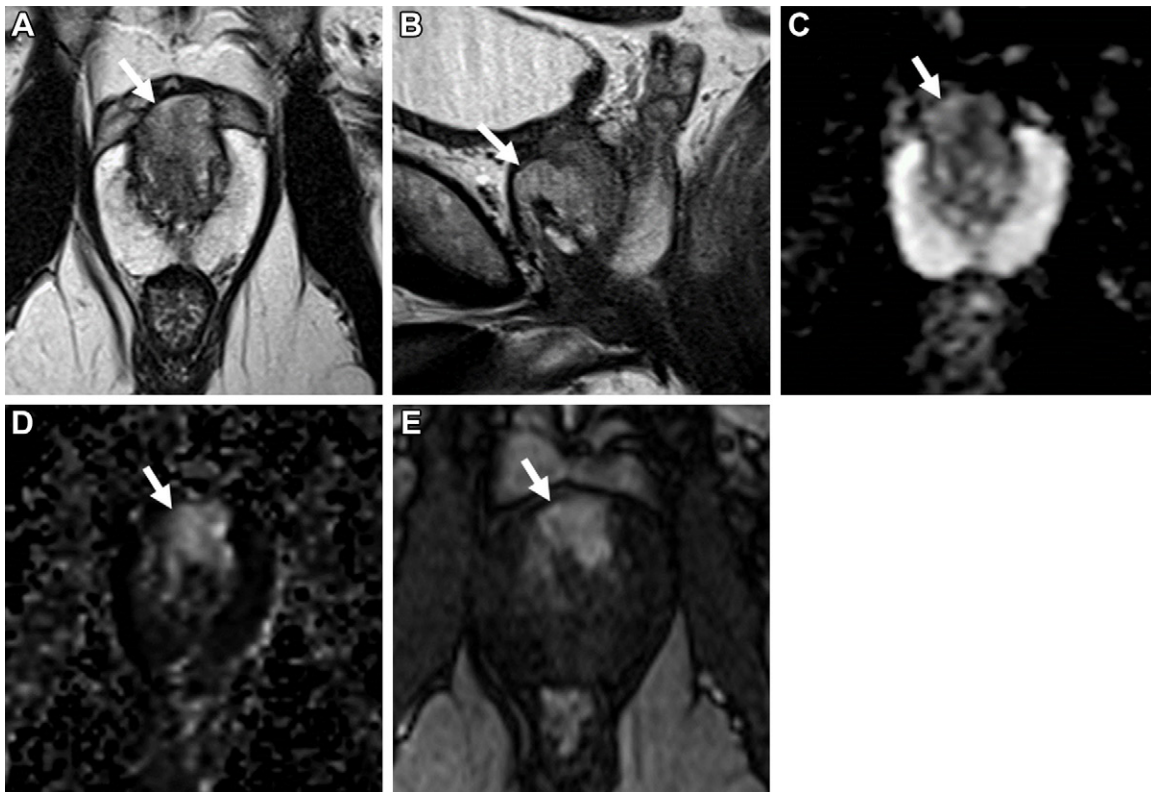


Figure 2: Images in a 68-year-old man with a prostate-specific antigen level of 21.8 ng/mL and a prior negative prostate biopsy. **(A)** Axial and **(B)** sagittal T2-weighted MRI scans show a lesion in the midline anterior transition zone at the mid gland, with intermediate to high signal intensity and anterior extraprostatic extension (arrows). **(C)** The apparent diffusion coefficient map shows diffusion restriction with moderately hypointense signal (arrow) within the lesion, while the **(D)** diffusion-weighted image with a high b value of 1400 sec/mm² shows moderately hyperintense signal (arrow); the **(E)** dynamic contrast-enhanced MRI scan shows corresponding early arterial enhancement (arrow). The signal intensity of the lesion at T2-weighted MRI is higher than expected for typical prostate adenocarcinoma, but because of the extraprostatic extension findings, the lesion was assigned a T2-weighted MRI and an overall Prostate Imaging Reporting and Data System score of 5. MRI-targeted biopsy of the lesion revealed Gleason 4+4 prostate cancer with predominate cribriform morphology.

In a multireader study, Winkel et al (28) evaluated the impact of a deep learning–based prostate AI model on the accuracy and efficiency of biparametric MRI (bpMRI) interpretation in 100 patients. Seven radiologists participated in two rounds of bpMRI interpretations, with and without AI. The AI model improved the radiologists’ performance in locating MRI-visible lesions, increasing the AUC from 0.84 to 0.88. Additionally, AI significantly improved the interreader agreement ($\kappa = 0.22$ without AI vs 0.36 with AI) and decreased the reading time by 21%, from 103 seconds to 81 ($P < .001$).

In another multireader study, Labus et al (29) evaluated the effect of a deep learning–based computer-aided detection system on experienced and less experienced radiologists reading prostate multiparametric MRI (mpMRI) to diagnose csPCa. With deep learning–based computer-aided detection assistance, the overall AUC of the less experienced radiologists increased significantly from 0.68 to 0.80 ($P = .002$).

In a feasibility study, Roest et al (30) showed that an AI model might identify changes in serial bpMRI, which can be particularly helpful in detecting csPCa in patients on active surveillance. The authors found that the performance of the AI model using the current and prior studies (AUC, 0.81) was better than the model using the current study alone (AUC, 0.73) and the

radiologist’s interpretation (AUC, 0.69). Interestingly, the model using current and prior studies further improved after adding clinical parameters (AUC, 0.86), highlighting the ability of AI models to handle different types of data.

Multiparametric versus Biparametric MRI

The current version of PI-RADS recommends mpMRI consisting of (a) T2-weighted imaging performed in the straight or oblique axial plane and at least one additional orthogonal plane (sagittal or coronal); (b) DWI performed with low– (0–100 sec/mm²), intermediate– (800–1000 sec/mm²), and high– (≥ 1400 sec/mm²) b value images and an ADC map; and (c) T1-weighted DCE imaging. The role of DCE MRI in the current PI-RADS is, however, limited to the characterization of peripheral zone lesions that receive a score of 3 at the DWI and ADC mapping (ie, mildly high signal intensity at DWI and mildly low signal intensity at ADC mapping, or markedly high signal intensity at DWI or markedly low signal intensity at ADC mapping, but not both). These peripheral zone lesions can be upgraded to a final PI-RADS category of 4 if they are positive at DCE imaging, which in PI-RADS version 2.1 is defined as “focal, and; earlier than or contemporaneously with enhancement of adjacent normal prostatic tissues, and;

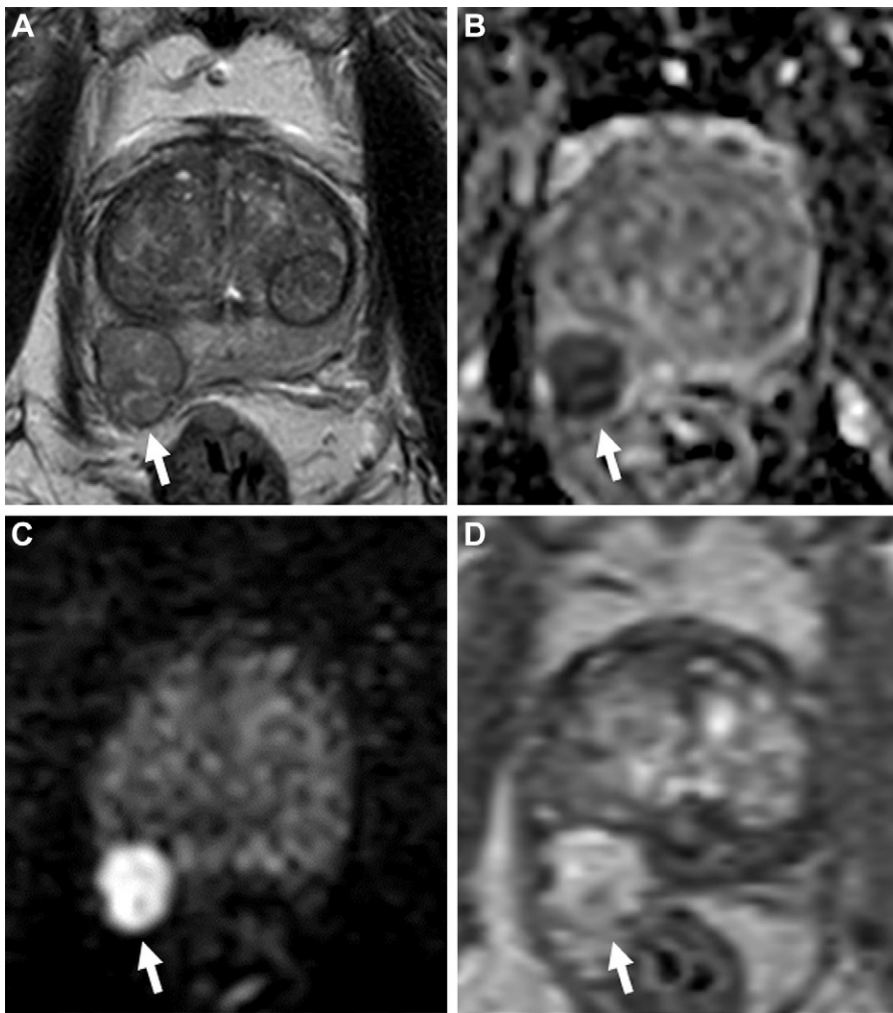


Figure 3: Images in a 78-year-old man with a serum prostate-specific antigen level of 10 ng/mL. **(A)** Axial T2-weighted MRI scan shows a well-encapsulated nodule in the right mid peripheral zone (arrow), which suggests an ectopic benign prostatic hyperplasia nodule. **(B)** The apparent diffusion coefficient map and **(C)** diffusion-weighted image with a b value of 1500 sec/mm^2 show the nodule with diffusion restriction with prominent hypointense and hyperintense signal features (arrows), and the **(D)** dynamic contrast-enhanced (DCE) MRI scan shows focal early enhancement (arrow). The T2-weighted imaging, diffusion-weighted imaging, DCE MRI, and overall Prostate Imaging Reporting and Data System scores of this lesion were 2, 5, positive, and 5, respectively. Transrectal US/MRI-fusion guided biopsy revealed Gleason 4+4 prostate cancer within this lesion.

In a retrospective study by Kuhl et al (33) using MRI-targeted biopsy as the reference standard, the diagnostic accuracy for the detection of csPCa was similar between the two techniques (bpMRI, 89.1%; mpMRI, 87.2%). While one additional csPCa was detected with the use of mpMRI compared with bpMRI (139 vs 138), mpMRI also led to 11 false-positive diagnoses. The detection of csPCa with use of the bpMRI protocol has since been evaluated in prospective studies (17), including a randomized clinical trial in the screening setting (15). These studies show that compared with systematic biopsy, MRI interpretation using PI-RADS scores

corresponds to suspicious finding on [T2-weighted imaging and/or DWI.]”

In such a role, DCE MRI can improve the stratification of the risk of lesions representing csPCa. Druskin et al (31) evaluated the impact of DCE MRI by comparing csPCa detection rates for PI-RADS category 3, category 3+1 (ie, DWI category 3 with DCE MRI positivity), and category 4 (ie, DWI category 4) peripheral zone lesions, with MRI-guided biopsy as the reference standard. The rates of csPCa for PI-RADS category 3, 3+1, and 4 lesions were 8.9%, 21%, and 36.5%, respectively ($P < .03$). The csPCa detection rate was higher in the PI-RADS 3+1 category compared with PI-RADS 3 category in the patients with prior negative systematic biopsy (28% vs 5.0%; $P < .001$) but not in biopsy-naïve patients. Greer et al (32) found that category 3+1 lesions in the peripheral zone also had a higher cancer likelihood than did category 3 lesions (67.8% vs 40.0%; $P = .02$) in a retrospective cohort of patients who underwent radical prostatectomy. Such benefit, however, does not seem to justify the routine use of DCE MRI, which is the most invasive and costly component of the mpMRI protocol, generally adding up to 10 minutes to the examination. Based on these arguments, in the past half-decade, bpMRI, which uses T2-weighted imaging and DWI and ADC mapping, has been suggested as an alternative.

without the DCE information followed by MRI-guided biopsy is at least noninferior for csPCa detection, has lower detection rates of insignificant cancers, and can decrease the number of unnecessary biopsies significantly. Considering these results and the increasing pressure to reduce health care expenditure, we anticipate that bpMRI adoption will increase and eventually become the standard of care in patients undergoing initial diagnostic work-up for PCa, and possibly for patients with PCa on active surveillance who may require serial imaging.

One important aspect of the current bpMRI literature is the exclusion of patients with nondiagnostic DWI examinations secondary to susceptibility artifacts from hip prostheses or geometric distortion by rectal gas. In such cases, DCE MRI can be a valuable safety net and assist in the diagnosis (Fig 8). Considering that these two conditions are common in the population imaged using prostate MRI, their results should be evaluated cautiously. Early research on alternative DWI techniques less susceptible to metal artifacts (34) and quantitative methods such as T2 mapping has shown promising results in this setting, but their use has not yet been subject to rigorous validation (35).

In 2021, the PI-RADS Steering Committee acknowledged that bpMRI represents a potential solution for meeting

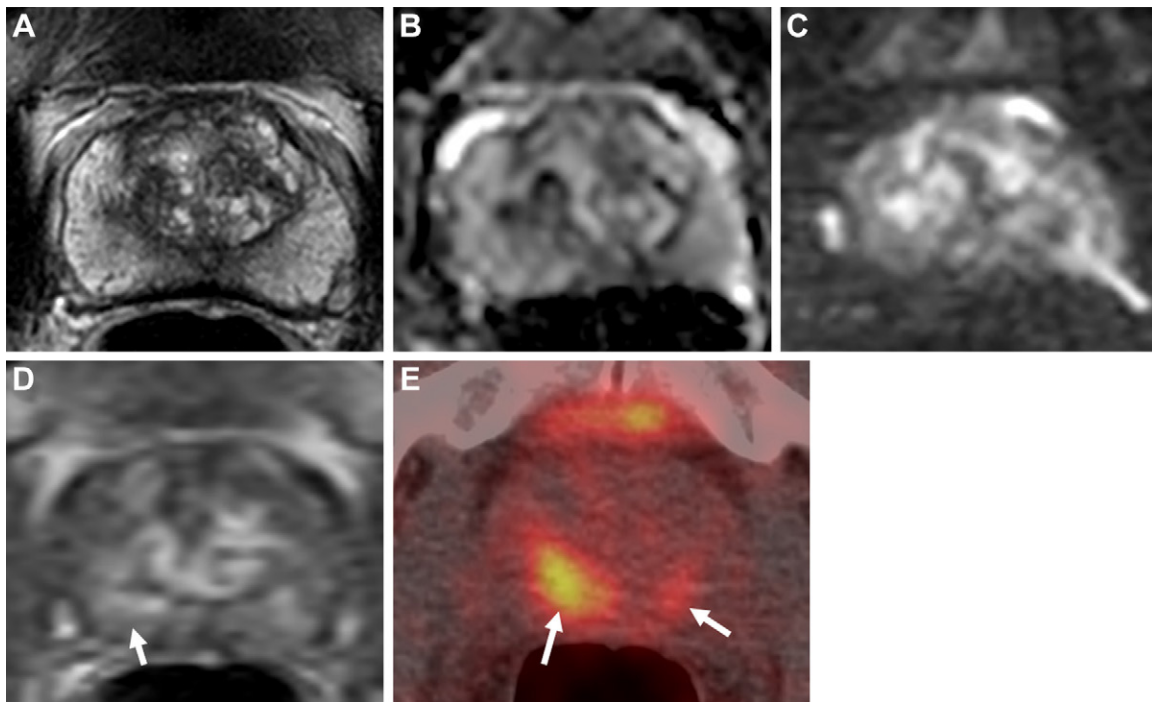


Figure 4: Images in a 74-year-old man with a serum prostate-specific antigen level of 12.9 ng/mL. **(A)** Axial T2-weighted MRI scan, **(B)** apparent diffusion coefficient map, and **(C)** diffusion-weighted image with a b value of 1500 sec/mm² demonstrate no focal lesion within the prostate gland. **(D)** Dynamic contrast-enhanced MRI scan shows a very subtle linear enhancement in the right mid peripheral zone (arrow). Overall, the multiparametric MRI examination was negative for a cancer-suspicious lesion according to the Prostate Imaging Reporting and Data System. **(E)** Axial fluorine 18 DCFPyl PET/CT image demonstrates bilateral uptake (greater on the right side) in the prostate (arrows). Prostate biopsy revealed Gleason 4+3 prostate cancer within the right mid peripheral zone. DCFPyl = 2-(3-[1-carboxy-5-[(6-¹⁸F-fluoro-pyridine-3-carbonyl)-amino]-pentyl]-ureido)-pentanedioic acid).

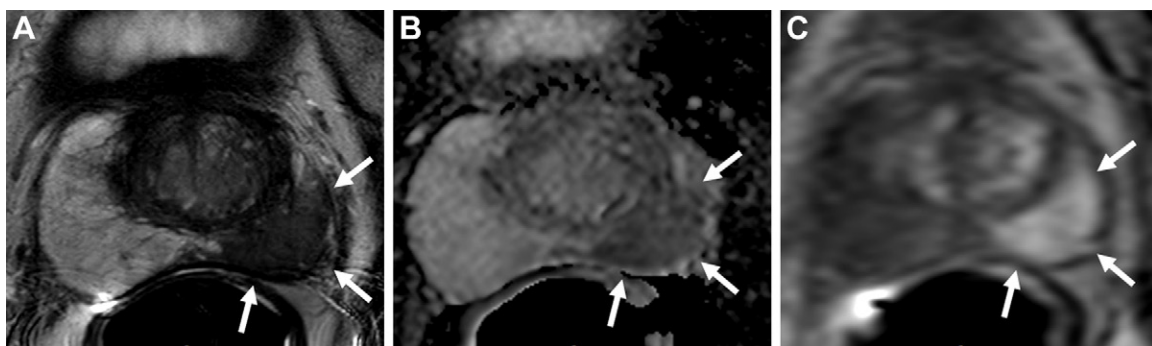


Figure 5: Images in a 61-year-old man with a serum prostate-specific antigen level of 8 ng/mL. **(A)** Axial T2-weighted MRI scan shows a large homogeneously hypointense lesion in the entire left peripheral zone (arrows). **(B)** The apparent diffusion coefficient map shows the lesion with mild to moderate diffusion restriction (arrows), and the **(C)** dynamic contrast-enhanced MRI scan shows focal early enhancement (arrows). The overall Prostate Imaging Reporting and Data System score of this lesion was 5. Transrectal US/MRI fusion-guided biopsy revealed chronic granulomatous prostatitis secondary to tuberculosis within this lesion.

the increasing demand for prostate MRI. They recommend that the advantages and disadvantages for operational workflow, radiologic assessment, and diagnostic performance be weighed carefully, considering the likelihood of csPCa being present and the clinical priorities of patients and their referrers. Additionally, they stated that optimal image acquisition and data interpretation are mandatory because there is likely a degradation of bpMRI performance in clinical practice. A major concern is that bpMRI may lead to an increased number of indeterminate lesions (ie, PI-RADS category 3), which

may result in decreased specificity of MRI and more uncertainty in the determination of the need for biopsy (36).

PI-RADS and Quality Control

There are valid concerns that the increased use of MRI could lead to variations in the quality of imaging acquisition and reporting. This is problematic because MRI quality influences all downstream events in the MRI-directed PCa diagnostic pathway (37). Previous reports from various groups have shown that adherence to PI-RADS technical standards for imaging

Table 1: PI-RADS T2-weighted MRI Peripheral Zone Categories Organized by Year and Version

PI-RADS Category	PI-RADS Year and Version		
	2012 (Version 1)	2015 (Version 2)	2019 (Version 2.1)
Category 1	Uniform high signal intensity	Uniform hyperintense signal intensity (normal)	Uniform hyperintense signal intensity (normal)
Category 2	Linear, wedge-shaped, or geographic areas of lower signal intensity, usually not well demarcated	Linear or wedge-shaped hypointensity or diffuse mild hypointensity, usually indistinct margin	Linear or wedge-shaped hypointensity or diffuse mild hypointensity, usually indistinct margin
Category 3	Intermediate appearances not in categories 1/2 or 4/5	Heterogeneous signal intensity or noncircumscribed, rounded, moderate hypointensity; includes others that do not qualify as 2, 4, or 5	Heterogeneous signal intensity or noncircumscribed, rounded, moderate hypointensity; includes others that do not qualify as 2, 4, or 5
Category 4	Discrete, homogeneous low signal focus/mass confined to the prostate	Circumscribed, homogeneous moderate hypointense focus/mass confined to prostate and <1.5 cm in greatest dimension	Circumscribed, homogeneous moderate hypointense focus/mass confined to prostate and <1.5 cm in greatest dimension
Category 5	Discrete, homogeneous low signal intensity focus with extracapsular extension/invasive behavior or mass effect on the capsule (bulging), or broad (>1.5 cm) contact with the surface	Same as 4 but ≥1.5 cm in greatest dimension or definite extraprostatic extension/invasive behavior	Same as 4 but ≥1.5 cm in greatest dimension or definite extraprostatic extension/invasive behavior

Note.—PI-RADS = Prostate Imaging Reporting and Data System.

Table 2: PI-RADS T2-weighted MRI TZ Categories Organized by Year and Version

PI-RADS Category	PI-RADS Year and Version		
	2012 (Version 1)	2015 (Version 2)	2019 (Version 2.1)
Category 1	Heterogeneous TZ adenoma with well-defined margins: “organized chaos”	Homogeneous intermediate signal intensity (normal)	Normal-appearing TZ (rare) or a round, completely encapsulated nodule (“typical nodule”)
Category 2	Areas of more homogeneous low signal intensity, however well marginated, originating from the TZ/BPH	Circumscribed hypointense or heterogeneous encapsulated nodule(s) (BPH)	A mostly encapsulated nodule OR a homogeneous circumscribed nodule without encapsulation (“atypical nodule”) OR a homogeneous mildly hypointense area between nodules
Category 3	Intermediate appearances not in categories 1/2 or 4/5	Heterogeneous signal intensity with obscured margins; includes others that do not qualify as 2, 4, or 5	Heterogeneous signal intensity with obscured margins; includes others that do not qualify as 2, 4, or 5
Category 4	Areas of more homogeneous low signal intensity, ill-defined: “erased charcoal sign”	Lenticular or noncircumscribed, homogeneous, moderately hypointense, and <1.5 cm in greatest dimension	Lenticular or noncircumscribed, homogeneous, moderately hypointense, and <1.5 cm in greatest dimension
Category 5	Same as 4 but involving the anterior fibromuscular stroma or the anterior horn of the peripheral zone, usually lenticular or water-drop shaped	Same as 4 but ≥1.5 cm in greatest dimension or definite extraprostatic extension/invasive behavior	Same as 4, but ≥1.5 cm in greatest dimension or definite extraprostatic extension/invasive behavior

Note.—BPH = benign prostatic hyperplasia, PI-RADS = Prostate Imaging Reporting and Data System, TZ = transition zone.

acquisition is inconsistent across sites and tends to be lower in nonacademic medical centers and centers that lack expertise in prostate MRI (38,39). Adherence to the standards is critical to improving the reproducibility of the examination and implementation of quantitative methods, although it only

sometimes translates into adequate image quality. This is due to (a) the intrinsic limitations of some scanners, especially older platforms and those with 1.5-T magnetic field strength, and (b) patient-specific factors (eg, large body size, metal implants, and lack of adequate bowel preparation).

Table 3: PI-RADS Diffusion-weighted MRI Categories Organized by Year and Version

PI-RADS Category	PI-RADS Year and Version		
	2012 (Version 1)	2015 (Version 2)	2019 (Version 2.1)
Category 1	No reduction in ADC compared with normal glandular tissue; no increase in signal intensity on any high <i>b</i> -value image ($\geq 800 \text{ sec/mm}^2$)	No abnormality (ie, normal) on ADC and high <i>b</i> -value DWI	No abnormality (ie, normal) on ADC and high <i>b</i> -value DWI
Category 2	Diffuse, hyperintense signal on $\geq 800 \text{ sec/mm}^2$ image with low ADC; no focal features, however, linear, triangular or geographical features are allowed	Indistinct hypointense on ADC	Linear/wedge-shaped hypointense on ADC and/or linear/wedge-shaped hyperintense on high <i>b</i> -value DWI
Category 3	Intermediate appearances not in categories 1/2 or 4/5	Focal mildly/moderately hypointense on ADC and isointense/mildly hyperintense on high <i>b</i> -value DWI	Focal (discrete and different from the background) hypointense on ADC and/or focal hyperintense on high <i>b</i> -value DWI; may be markedly hypointense on ADC or markedly hyperintense on high <i>b</i> -value DWI, but not both
Category 4	Focal area(s) of reduced ADC but isointense signal intensity on high <i>b</i> -value images ($\geq 800 \text{ sec/mm}^2$)	Focal markedly hypointense on ADC and markedly hyperintense on high <i>b</i> -value DWI; $< 1.5 \text{ cm}$ in greatest dimension	Focal markedly hypointense on ADC and markedly hyperintense on high <i>b</i> -value DWI; $< 1.5 \text{ cm}$ in greatest dimension
Category 5	Focal area/mass of hyperintense signal on the high <i>b</i> -value images ($\geq 800 \text{ sec/mm}^2$) with reduced ADC	Same as 4 but $\geq 1.5 \text{ cm}$ in greatest dimension or definite extraprostatic extension/invasive behavior	Same as 4 but $\geq 1.5 \text{ cm}$ in greatest dimension or definite extraprostatic extension/invasive behavior

Note.—ADC = apparent diffusion coefficient, DWI = diffusion-weighted imaging, PI-RADS = Prostate Imaging Reporting and Data System.

Table 4: PI-RADS DCE MRI Categories Organized by Year and Version

	2012 (Version 1)	2015 (Version 2)	2019 (Version 2.1)
Category 1	Type 1 enhancement curve	Negative	Negative
Category 2	Type 2 enhancement curve	No early enhancement, or diffuse enhancement not corresponding to a focal finding on T2-weighted imaging and/or DWI or focal enhancement corresponding to a lesion demonstrating features of BPH on T2-weighted imaging	No early or contemporaneous enhancement; or diffuse multifocal enhancement NOT corresponding to a focal finding on T2-weighted imaging and/or DWI or focal enhancement corresponding to a lesion demonstrating features of BPH on T2-weighted imaging (including features of extruded BPH in the peripheral zone)
Category 3	Type 3 enhancement curve	Positive	Positive
Extra rules	+1 for focal enhancing lesion with curve type 2–3; +1 for asymmetric lesion or lesion at an unusual place with curve type 2–3	Focal, and; earlier than or contemporaneously with enhancement of adjacent normal prostatic tissues, and corresponds to suspicious finding on T2-weighted imaging and/or DWI	Focal, and; earlier than or contemporaneously with enhancement of adjacent normal prostatic tissues, and; corresponds to suspicious finding on T2-weighted imaging and/or DWI

Note.—BPH = benign prostatic hyperplasia, DCE = dynamic contrast-enhanced, DWI = diffusion-weighted imaging, PI-RADS = Prostate Imaging Reporting and Data System.

In a retrospective study that included examinations from 62 patients performed at various imaging centers, T2-weighted imaging and DWI were considered to have adequate diagnostic quality in the same examination in only 56% of cases (40). The

adherence to PI-RADS version 2 technical standards also varied widely. Moreover, a correlation between adherence to the technical standards and image quality or diagnostic adequacy was not observed for DWI and was weak for T2-weighted imaging. The

study also found that reader agreement on image quality was poor in T2-weighted imaging ($\kappa = 0.17$) and only fair in DWI ($\kappa = 0.21$), despite initial training of the readers by an expert in prostate MRI. This highlights the difficulty in determining what constitutes a “good quality” examination.

Since then, the Prostate Image Quality (PI-QUAL) system has been developed to describe the adequacy of images regarding technical standards compliance and the presence of artifacts that negatively affect image interpretation. In this five-point scale system, the final score is based on the number of MRI pulse sequences that are optimal or have adequate diagnostic quality to rule in and rule out all csPCa. For a PI-QUAL score of 1, none of the sequences have sufficient diagnostic quality, and therefore all clinically significant lesions cannot be ruled in or ruled out, while for a PI-QUAL score of 5, the three sequences are of optimal quality, and hence all clinically significant lesions can be ruled in and ruled out (41,42). The system represented an important step toward developing standards for image quality. Still, more data are needed to demonstrate the correlation between adherence to technical standards and other qualitative image quality parameters with the true diagnostic capability of MRI. This information will be critical for guiding the PI-RADS Steering Committee on what aspects of technical standards need to be modified in future iterations of PI-RADS.

Thus far, research has shown that the percentage of indeterminate MRI results (ie, PI-RADS category 3) decreased with increasing image quality, from 31.8% for PI-QUAL 3 to 12.5% for PI-QUAL 4 and 10.4% for PI-QUAL 5 (43). Other researchers found that in studies with a PI-QUAL score of 5, the negative MRI calls (without discriminating true-negative studies from false-negative studies) increased from 50% to 87%, and the PI-RADS category 3 rates decreased from 31.8% to 10.4% compared with PI-QUAL 3 studies. More patients with images with PI-QUAL scores of 3 or less underwent biopsy for negative MRI scans (PI-RADS category 1 or 2 [47%]) and indeterminate MRI scans (PI-RADS 3 [100%]) compared with a PI-QUAL score of 4 or 5 (30% and 75%, respectively) (43). Similarly, other studies found that patients with an MRI examination rated with a PI-QUAL score of 3

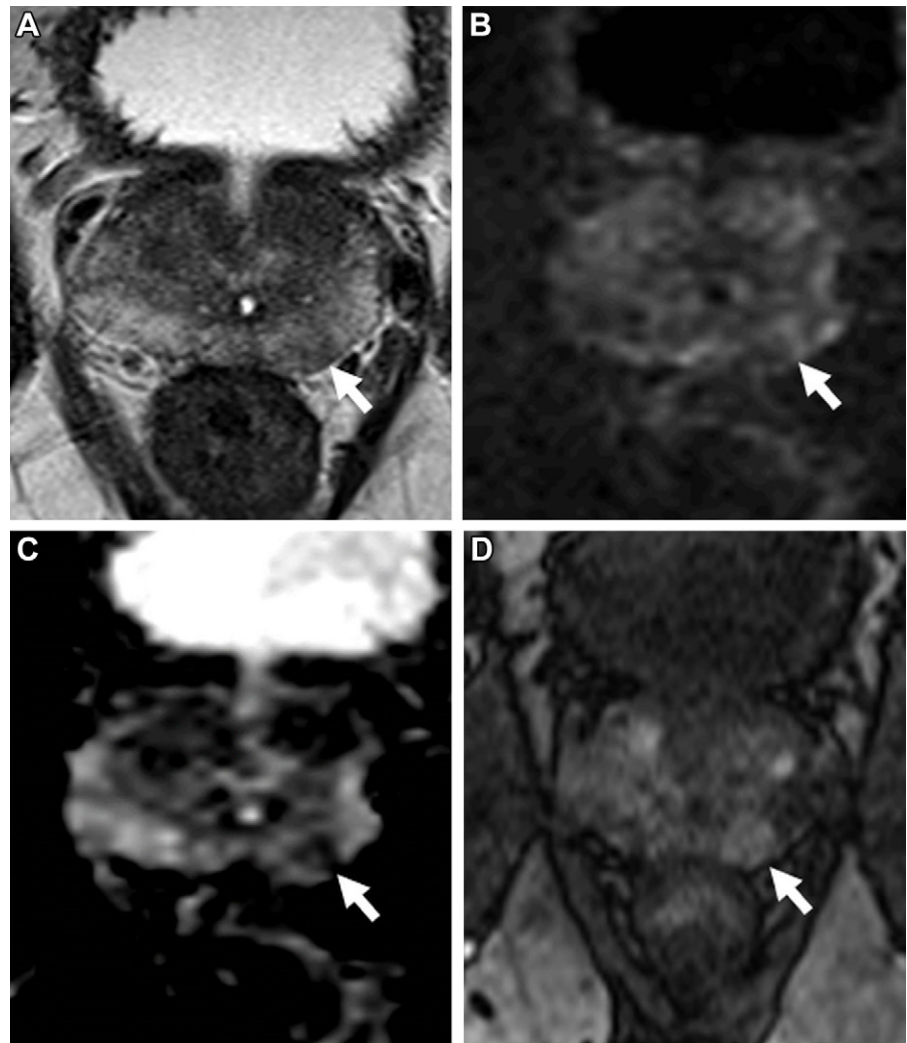


Figure 6: Images in a 59-year-old man with a prostate-specific antigen level of 2.9 ng/mL and a prior negative prostate biopsy. **(A)** Axial T2-weighted MRI scan shows a subtle, noncircumscribed, moderately hypointense focus in the left base posteromedial peripheral zone (arrow) [T2-weighted MRI Prostate Imaging Reporting and Data System [PI-RADS] score of 3]. On the **(B)** axial diffusion-weighted image with a high b value (1400 sec/mm²), the lesion has ill-defined mildly hyperintense signal (arrow), and on the **(C)** apparent diffusion coefficient (ADC) map, it has markedly hypointense signal (arrow) (diffusion-weighted imaging and ADC PI-RADS score of 3). On the **(D)** dynamic contrast-enhanced (DCE) MRI scan, the lesion shows early contrast enhancement (arrow) (DCE MRI PI-RADS score of positive). The final assessment category assigned was PI-RADS category 4. The focal abnormality was not identified at the time of the MRI interpretation by a novice reader, who assigned PI-RADS category 2 to the examination. Upon review of the images by a more experienced reader, the lesion was identified, and an MRI-targeted biopsy of the lesion revealed prostate cancer with a Gleason score of 3+4.

or less had lower csPCa detection rates at MRI-guided biopsy. This suggests that poor-quality scans can lead to more false-positive examinations, jeopardizing one of the main benefits of using MRI to triage patients for biopsy, which is to decrease the number of unnecessary biopsies (44). Alternatively, it is also conceivable that poor-quality examinations miss csPCa that is not detected with systematic biopsies. Preliminary data also suggest that interreader variability of PI-RADS categorization is higher on examinations with lower PI-QUAL scores, underscoring the impact of image quality on examination interpretation (45).

Beyond imaging interpretation, image quality can influence other aspects of PCa diagnosis with MRI. Susceptibility artifacts from rectal gas can compromise the quantitative information

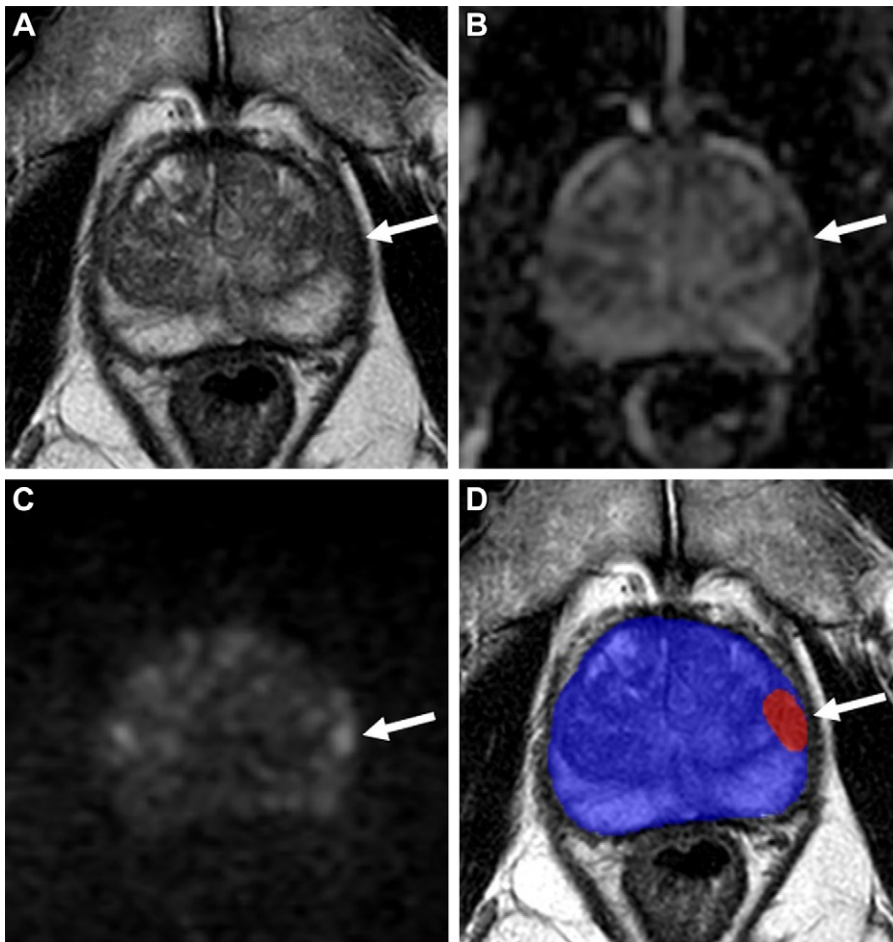


Figure 7: Images in a 72-year-old man with a serum prostate-specific antigen level of 8.95 ng/mL. **(A)** Axial T2-weighted MRI scan shows a focal hypointense lesion in the left apical-mid anterior peripheral zone (arrow). **(B)** Apparent diffusion coefficient map and **(C)** diffusion-weighted image with a b value of 1500 sec/mm² show the lesion with mild to moderate diffusion restriction (arrows). **(D)** Biparametric MRI-based artificial intelligence model's binary prediction map overlaid on the T2-weighted MRI scan automatically segments the prostate gland (blue shading) and detects the same lesion that was shown in other sequences (arrow; red shading). Transrectal US/MRI fusion-guided biopsy revealed Gleason 3+4 prostate cancer within this lesion.

generated by DWI and ADC maps. Motion-related artifacts can not only hamper the detection and staging of lesions but also make the segmentation of the prostate gland and the creation of targets for MRI/US fusion-guided biopsy less efficient and potentially less accurate.

Rigorous processes for outcome analysis of prostate MRI results leveraging the structured reporting approach embedded in PI-RADS have been reported (46). Such a framework enables the development of both system- and provider-level performance improvement efforts by highlighting sources of variation and offers an opportunity to improve future iterations of PI-RADS. Researchers have shown that subspecialty-trained abdominal radiologists with a wide range of experience can obtain consistent positive predictive values for PI-RADS version 2 categories 3–5 (46). These studies, along with meta-analyses, help establish the ranges of risk associated with each PI-RADS category, akin to the Breast Imaging Reporting and Data System categories, even though they can be influenced by nonimaging features, such as family history of PCa or genetic variations. These benchmarks, in turn, can be used to counsel

patients about needing a biopsy and serve as quality metrics for individual prostate MRI readers, urologists, or radiologists performing the biopsies and for medical centers. The recently established American College of Radiology Prostate Cancer MRI Center designation requires sites to develop mechanisms for follow-up on biopsy results, highlighting the need to monitor the effectiveness of prostate MRI programs.

PI-RADS beyond PCa Detection and MRI

Studies have shown that the MRI phenotypes of PCa, according to the PI-RADS assessment categories, have prognostic value and can be used as biomarkers for more aggressive forms of PCa, independent of their correlation with histopathologic findings (47,48). Patients with PI-RADS category 4 or 5 lesions are more likely to develop biochemical recurrence after PCa treatment and more likely to experience metastasis and PCa-specific death (48). Based on these findings, PI-RADS scores may eventually play a more prominent role in patient management beyond determining the need for a biopsy. For instance, the FLAME (Focal Lesion Ablative Microboost in Prostate Cancer) multicenter randomized clinical trial showed that patients who received a radiation

boost in intraprostatic MRI-visible lesions had significantly higher biochemical recurrence-free survival than those who received standard radiation. These findings align with those from Gorovets et al (49), who showed that local recurrences after radiation treatment occur mainly in the location of the dominant PI-RADS category 4 or 5 lesions.

Other scoring systems have also emerged in the past half-decade to address indications for prostate MRI not covered by PI-RADS. These include the National Cancer Institute grading system for extraprostatic extension (50), the Prostate Magnetic Resonance Imaging for Local Recurrence Reporting guidelines (51), and the Prostate Cancer Radiological Estimation of Change in Sequential Evaluation, or PRECISE, criteria for serial mpMRI of the prostate during active surveillance (52). While these systems have yet to be widely adopted, their performance has been investigated, with promising results (53,54).

Scoring systems have also been developed for other imaging modalities. The Prostate Risk Identification Using Micro-US protocol was created to describe findings on

high-resolution US images generated by 29-MHz transducers (55), an alternative method for PCa diagnosis in patients who do not have access or have contraindications to MRI (56). The PRIMARY score is a framework for classifying intraprostatic findings on prostate-specific membrane antigen–targeted PET scans into categories that reflect the likelihood of the presence of csPCa (57). Like PI-RADS, these systems aim to standardize communication among health care providers, both in research and in the delivery of patient care. Integration of these systems with PI-RADS could increase their usage and help harmonize the results from the different modalities that may have complementary roles, particularly when the finding at either imaging technique is negative or equivocal, as it is currently done with breast (Breast Imaging Reporting and Data System, or BI-RADS) and liver imaging (Liver Imaging Reporting and Data System, or LI-RADS).

Where Next?

In just over a decade, PI-RADS has evolved from a European consensus to a robust global standard for prostate MRI acquisition, interpretation, and reporting, leading to its inclusion in medical society guidelines (9). Overreliance on subjective parameters for imaging interpretation is a recognized limitation of PI-RADS that can be addressed using emerging quantitative MRI methods, prediction models incorporating clinical data, and sophisticated AI systems under development. With a growing interest in using abbreviated imaging protocols to keep up with the demand for prostate MRI, these solutions will become increasingly important but also require greater adoption of quality control methods to identify and mitigate sources of variation in system performance.

The evidence supporting novel approaches is accumulating, but limitations and barriers to their implementation in clinical practice are recognized. The overwhelming majority of the studies evaluating these approaches are retrospective and based on small cohorts of patients lacking ethnic diversity, often performed at a single or a few centers, where the level of expertise is superior to that of most practices. Moreover, variability in MRI technical parameters—such as b value selection, which influences apparent diffusion coefficient map calculations—also limits the

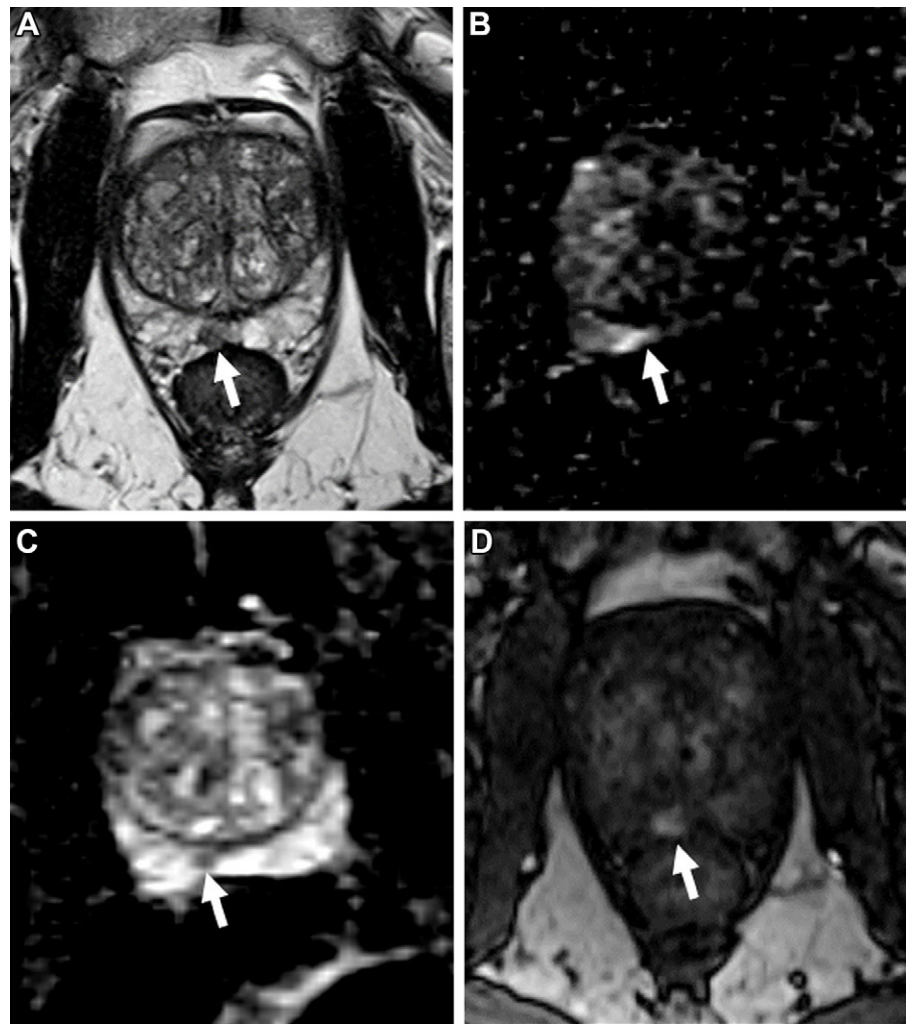


Figure 8: Images in a 65-year-old man with a prostate-specific antigen level of 3.4 ng/mL and no prior biopsy. **(A)** Axial T2-weighted MRI scan shows a 0.6-cm focal lesion with hypointense signal in the right mid posteromedial peripheral zone (arrow) (T2-weighted MRI Prostate Imaging Reporting and Data System [PI-RADS] score of 4). **(B)** Axial diffusion-weighted image with a high b value of 1400 sec/mm² shows susceptibility artifacts from rectal gas (arrow), causing geometric distortion that makes it difficult to categorize the lesion. **(C)** The apparent diffusion coefficient map shows the lesion with a markedly hypointense signal (arrow), and it is not as distorted as at diffusion-weighted imaging. **(D)** Dynamic contrast-enhanced (DCE) MRI scan shows early focal contrast enhancement within this lesion (arrow) (DCE MRI PI-RADS score of positive). The DCE image helped confirm the finding on the T2-weighted image and assign a final assessment category, since at least two of the three sequences must have sufficient diagnostic quality to give a Prostate Imaging Reporting and Data System score. MRI-targeted biopsy of the lesion revealed prostate cancer with a Gleason score of 3+4.

generalizability of their results. Robust data sets with ground truth based on accurate histopathologic annotations, including those made available through recent prostate MRI artificial intelligence challenges, will be critical for developing prediction algorithms for prostate cancer detection at MRI (58,59). It is currently unknown when the next version of the Prostate Imaging Reporting and Data System (PI-RADS) will be released. For now, all we need to do is join a very active research community on PI-RADS, since future iterations of the system depend on high-quality studies that address the limitations of the current literature.

Disclosures of conflicts of interest: B.T. Cooperative research and development agreements with NVIDIA and Philips; royalties from the National Institutes of Health; patents in the field of artificial intelligence. A.S.P. Grants to institution

from the American College of Radiology, Profound Medical, and Blue Earth Diagnostics; consulting fees from Koelis.

References

- Steyn JH, Smith FW. Nuclear magnetic resonance imaging of the prostate. *Br J Urol* 1982;54(6):726–728.
- Westphalen AC, McCulloch CE, Anaokar JM, et al. Variability of the positive predictive value of PI-RADS for prostate MRI across 26 centers: experience of the Society of Abdominal Radiology Prostate Cancer Disease-focused Panel. *Radiology* 2020;296(1):76–84.
- Kelloff GJ, Choyke P, Coffey DS; Prostate Cancer Imaging Working Group. Challenges in clinical prostate cancer: role of imaging. *AJR Am J Roentgenol* 2009;192(6):1455–1470.
- Dickinson L, Ahmed HU, Allen C, et al. Magnetic resonance imaging for the detection, localisation, and characterisation of prostate cancer: recommendations from a European consensus meeting. *Eur Urol* 2011;59(4):477–494.
- Barentsz JO, Richenberg J, Clements R, et al. ESUR prostate MR guidelines 2012. *Eur Radiol* 2012;22(4):746–757.
- Weinreb JC, Barentsz JO, Choyke PL, et al. PI-RADS Prostate Imaging - Reporting and Data System: 2015, Version 2. *Eur Urol* 2016;69(1):16–40.
- Zhang L, Tang M, Chen S, Lei X, Zhang X, Huan Y. A meta-analysis of use of Prostate Imaging Reporting and Data System version 2 (PI-RADS V2) with multiparametric MR imaging for the detection of prostate cancer. *Eur Radiol* 2017;27(12):5204–5214.
- Turkbey B, Rosenkrantz AB, Haider MA, et al. Prostate Imaging Reporting and Data System Version 2.1: 2019 Update of Prostate Imaging Reporting and Data System Version 2. *Eur Urol* 2019;76(3):340–351.
- European Association of Urology. Prostate Cancer Guidelines. <https://uroweb.org/guidelines/prostate-cancer>. Accessed December 7, 2022.
- Eastham JA, Auffenberg GB, Barocas DA, et al. Clinically localized prostate cancer: AUA/ASTRO guideline, part I: introduction, risk assessment, staging, and risk-based management. *J Urol* 2022;208(1):10–18.
- Kasivivanathan V, Rannikko AS, Borghi M, et al. MRI-targeted or standard biopsy for prostate-cancer diagnosis. *N Engl J Med* 2018;378(19):1767–1777.
- Klotz L, Chin J, Black PC, et al. Comparison of multiparametric magnetic resonance imaging-targeted biopsy with systematic transrectal ultrasonography biopsy for biopsy-naïve men at risk for prostate cancer: a phase 3 randomized clinical trial. *JAMA Oncol* 2021;7(4):534–542.
- Eklund M, Jäderling F, Discacciati A, et al. MRI-targeted or standard biopsy in prostate cancer screening. *N Engl J Med* 2021;385(10):908–920.
- Hugosson J, Månsson M, Wallström J, et al. Prostate cancer screening with PSA and MRI followed by targeted biopsy only. *N Engl J Med* 2022;387(23):2126–2137.
- Hao S, Discacciati A, Eklund M, et al. Cost-effectiveness of prostate cancer screening using magnetic resonance imaging or standard biopsy based on the STHLM3-MRI study. *JAMA Oncol* 2022;9(1):88–94.
- Johnson DC, Raman SA, Miral SA, et al. Detection of individual prostate cancer foci via multiparametric magnetic resonance imaging. *Eur Urol* 2019;75(5):712–720.
- Sonni I, Felker ER, Lenis AT, et al. Head-to-head comparison of ⁶⁸Ga-PSMA-11 PET/CT and mpMRI with a histopathology gold standard in the detection, intraprostatic localization, and determination of local extension of primary prostate cancer: results from a prospective single-center imaging trial. *J Nucl Med* 2022;63(6):847–854.
- Radtke JB, Wiesenfarth M, Kesch C, et al. Combined clinical parameters and multiparametric magnetic resonance imaging for advanced risk modeling of prostate cancer—patient-tailored risk stratification can reduce unnecessary biopsies. *Eur Urol* 2017;72(6):888–896.
- Mehralivand S, Shih JH, Rais-Bahrami S, et al. A magnetic resonance imaging-based prediction model for prostate biopsy risk stratification. *JAMA Oncol* 2018;4(5):678–685.
- Stevens E, Truong M, Bullen JA, Ward RD, Purysko AS, Klein EA. Clinical utility of PSAD combined with PI-RADS category for the detection of clinically significant prostate cancer. *Urol Oncol* 2020;38(11):846.e9–846.e16.
- Deniffel D, Healy GM, Dong X, et al. Avoiding unnecessary biopsy: MRI-based risk models versus a PI-RADS and PSA density strategy for clinically significant prostate cancer. *Radiology* 2021;300(2):369–379.
- Tamada T, Huang C, Ream JM, Taffel M, Taneja SS, Rosenkrantz AB. Apparent diffusion coefficient values of prostate cancer: comparison of 2D and 3D ROIs. *AJR Am J Roentgenol* 2018;210(1):113–117.
- Gaur S, Harmon S, Rosenblum L, et al. Can apparent diffusion coefficient values assist PI-RADS version 2 DWI scoring? A correlation study using the PI-RADSV2 and International Society of Urological Pathology Systems. *AJR Am J Roentgenol* 2018;211(1):W33–W41.
- Tavakoli AA, Hielscher T, Badura P, et al. Contribution of dynamic contrast-enhanced and diffusion MRI to PI-RADS for detecting clinically significant prostate cancer. *Radiology* 2023;306(1):186–199.
- Greer MD, Lay N, Shih JH, et al. Computer-aided diagnosis prior to conventional interpretation of prostate mpMRI: an international multi-reader study. *Eur Radiol* 2018;28(10):4407–4417.
- Syer T, Mehta P, Antonelli M, et al. Artificial intelligence compared to radiologists for the initial diagnosis of prostate cancer on magnetic resonance imaging: a systematic review and recommendations for future studies. *Cancers (Basel)* 2021;13(13):3318.
- Cacciamani GE, Sanford DI, Chu TN, et al. Is artificial intelligence replacing our radiology stars? Not yet! *Eur Urol Open Sci* 2022;48:14–16.
- Winkel DJ, Tong A, Lou B, et al. A novel deep learning based computer-aided diagnosis system improves the accuracy and efficiency of radiologists in reading biparametric magnetic resonance images of the prostate: results of a multireader, multicase study. *Invest Radiol* 2021;56(10):605–613.
- Labus S, Altmann MM, Huisman H, et al. A concurrent, deep learning-based computer-aided detection system for prostate multiparametric MRI: a performance study involving experienced and less-experienced radiologists. *Eur Radiol* 2023;33(1):64–76.
- Roest C, Kwee TC, Saha A, Fütterer JJ, Yakar D, Huisman H. AI-assisted biparametric MRI surveillance of prostate cancer: feasibility study. *Eur Radiol* 2023;33(1):89–96.
- Druskin SC, Ward R, Purysko AS, et al. Dynamic contrast enhanced magnetic resonance imaging improves classification of prostate lesions: a study of pathological outcomes on targeted prostate biopsy. *J Urol* 2017;198(6):1301–1308.
- Greer MD, Shih JH, Lay N, et al. Validation of the dominant sequence paradigm and role of dynamic contrast-enhanced imaging in PI-RADS version 2. *Radiology* 2017;285(3):859–869.
- Kuhl CK, Bruhn R, Krämer N, Nebelung S, Heidenreich A, Schrading S. Abbreviated biparametric prostate MR imaging in men with elevated prostate-specific antigen. *Radiology* 2017;285(2):493–505.
- Hosseiny M, Sung KH, Felker E, et al. Read-out segmented echo planar imaging with two-dimensional navigator correction (RESOLVE): an alternative sequence to improve image quality on diffusion-weighted imaging of prostate. *Br J Radiol* 2022;95(1136):20211165.
- Sathiadoss P, Schieda N, Haroon M, et al. Utility of quantitative T2-mapping compared to conventional and advanced diffusion weighted imaging techniques for multiparametric prostate MRI in men with hip prosthesis. *J Magn Reson Imaging* 2022;55(1):265–274.
- Schoots IG, Barentsz JO, Bittencourt LK, et al. PI-RADS Committee position on MRI without contrast medium in biopsy-naïve men with suspected prostate cancer: narrative review. *AJR Am J Roentgenol* 2021;216(1):3–19.
- Barrett T, de Rooij M, Giganti F, Allen C, Barentsz JO, Padhani AR. Quality checkpoints in the MRI-directed prostate cancer diagnostic pathway. *Nat Rev Urol* 2023;20(1):9–22.
- Abreu-Gomez J, Shabana W, McInnes MDF, O'Sullivan JP, Morash C, Schieda N. Regional standardization of prostate multiparametric MRI performance and reporting: is there a role for a director of prostate imaging? *AJR Am J Roentgenol* 2019;213(4):844–850.
- Papoutsaki MV, Allen C, Giganti F, et al. Standardisation of prostate multiparametric MRI across a hospital network: a London experience. *Insights Imaging* 2021;12(1):52.
- Sackett J, Shih JH, Reese SE, et al. Quality of prostate MRI: is the PI-RADS standard sufficient? *Acad Radiol* 2021;28(2):199–207.
- Giganti F, Cole AP, Fennessy FM, et al. Promoting the use of the PI-QUAL score for prostate MRI quality: results from the ESOR Nicholas Gourtsoyianis teaching fellowship. *Eur Radiol* 2023;33(1):461–471.
- Giganti F, Allen C, Emberton M, Moore CM, Kasivivanathan V; PRECISION study group. Prostate Imaging Quality (PI-QUAL): a new quality control scoring system for multiparametric magnetic resonance imaging of the prostate from the PRECISION trial. *Eur Urol Oncol* 2020;3(5):615–619.
- Karanasios E, Caglic I, Zawaideh JP, Barrett T. Prostate MRI quality: clinical impact of the PI-QUAL score in prostate cancer diagnostic work-up. *Br J Radiol* 2022;95(1133):20211372.
- Pötsch N, Rainer E, Clauser P, et al. Impact of PI-QUAL on PI-RADS and cancer yield in an MRI-TRUS fusion biopsy population. *Eur J Radiol* 2022;154:110431.
- Giometti R, Blandino A, Zichichi C, et al. Inter-reader agreement of the Prostate Imaging Quality (PI-QUAL) score: a bicentric study. *Eur J Radiol* 2022;150:110267.
- Davenport MS, Downs E, George AK, et al. Prostate Imaging and Data Reporting System version 2 as a radiology performance metric: an analysis of 18 abdominal radiologists. *J Am Coll Radiol* 2021;18(8):1069–1076.

47. Stabile A, Mazzone E, Cirulli GO, et al. Association between multiparametric magnetic resonance imaging of the prostate and oncological outcomes after primary treatment for prostate cancer: a systematic review and meta-analysis. *Eur Urol Oncol* 2021;4(4):519–528.
48. Wibmer AG, Lefkowitz RA, Lakhman Y, et al. MRI-detectability of clinically significant prostate cancer relates to oncologic outcomes after prostatectomy. *Clin Genitourin Cancer* 2022;20(4):319–325.
49. Gorovets D, Wibmer AG, Moore A, et al. Local failure after prostate SBRT predominantly occurs in the PI-RADS 4 or 5 dominant intraprostatic lesion. *Eur Urol Oncol* 2022. 10.1016/j.euo.2022.02.005. Published online March 17, 2022.
50. Mehralivand S, Shih JH, Harmon S, et al. A grading system for the assessment of risk of extraprostatic extension of prostate cancer at multiparametric MRI. *Radiology* 2019;290(3):709–719.
51. Panebianco V, Villeirs G, Weinreb JC, et al. Prostate Magnetic Resonance Imaging for Local Recurrence Reporting (PI-RR): international consensus-based guidelines on multiparametric magnetic resonance imaging for prostate cancer recurrence after radiation therapy and radical prostatectomy. *Eur Urol Oncol* 2021;4(6):868–876.
52. Moore CM, Giganti F, Albertsen P, et al. Reporting magnetic resonance imaging in men on active surveillance for prostate cancer: the PRECISE recommendations—a report of a European School of Oncology Task Force. *Eur Urol* 2017;71(4):648–655.
53. Giganti F, Aupin L, Thoumin C, et al. Promoting the use of the PRECISE score for prostate MRI during active surveillance: results from the ESOR Nicholas Gourtsiannis teaching fellowship. *Insights Imaging* 2022;13(1):111.
54. Pecoraro M, Turkbey B, Purysko AS, et al. Diagnostic accuracy and observer agreement of the MRI Prostate Imaging for Recurrence Reporting Assessment score. *Radiology* 2022;304(2):342–350.
55. Ghai S, Eure G, Fradet V, et al. Assessing cancer risk on novel 29 MHz micro-ultrasound images of the prostate: creation of the micro-ultrasound protocol for prostate risk identification. *J Urol* 2016;196(2):562–569.
56. Ghai S, Perlis N, Atallah C, et al. Comparison of micro-US and multiparametric MRI for prostate cancer detection in biopsy-naive men. *Radiology* 2022;305(2):390–398.
57. Rowe SP, Gorin MA, Hammers HJ, et al. Imaging of metastatic clear cell renal cell carcinoma with PSMA-targeted ¹⁸F-DCFPyL PET/CT. *Ann Nucl Med* 2015;29(10):877–882.
58. Armato SG 3rd, Huisman H, Drukker K, et al. PROSTATEx Challenges for computerized classification of prostate lesions from multiparametric magnetic resonance images. *J Med Imaging (Bellingham)* 2018;5(4):044501.
59. The PI-CAI Challenge. <https://pi-cai.grand-challenge.org>. Accessed December 7, 2022.